Journal of Sound and Vibration 329 (2010) 3621–3631

Contents lists available at ScienceDirect

Journal of Sound and Vibration

journal homepage: www.elsevier.com/locate/jsvi

Rapid Communications

Response of uni-modal duffing-type harvesters to random forced excitations

Mohammed F. Daqaq

Nonlinear Vibrations and Energy Harvesting Lab. (NoVEHL), Department of Mechanical Engineering, Clemson University, Clemson, SC 29634, USA

ARTICLE INFO

Article history:
Received 13 November 2009
Received in revised form
5 April 2010
Accepted 6 April 2010
Handling Editor: L.N. Virgin
Available online 24 April 2010

ABSTRACT

Linear energy harvesters have a narrow frequency bandwidth and hence operate efficiently only when the excitation frequency is very close to the fundamental frequency of the harvester. Consequently, small variations of the excitation frequency around the harvester's fundamental frequency drops its small energy output even further making the energy harvesting process inefficient. To extend the harvester's bandwidth, some recent solutions call for utilizing energy harvesters with stiffness-type nonlinearities. From a steady-state perspective, this hardening-type nonlinearity can extend the coupling between the excitation and the harvester to a wider range of frequencies. In this effort, we investigate the response of such harvesters, which can be modeled as a uni-modal duffing-type oscillator, to White Gaussian and Colored excitations. For White excitations, we solve the Fokker–Plank–Kolmogorov equation for the exact joint probability density function of the response. We show that the expected value of the output power is not even a function of the nonlinearity. As such, under White excitations, nonlinearities in the stiffness do not provide any enhancement over the typical linear harvesters. We also demonstrate that nonlinearities in the damping and inertia may be used to enhance the expected value of the output power. For Colored excitations, we use the Van Kampen expansion and long-time numerical integration to investigate the influence of the nonlinearity on the expected value of the output power. We demonstrate that, regardless of the bandwidth or the center frequency of the excitation, the expected value of the output power decreases with the nonlinearity. With such findings, we conclude that energy harvesters modeled as uni-modal duffing-type oscillators are not good candidates for harvesting energy under forced random excitations. Using a linear transformation, results can be extended to the base excitation case.

1. Introduction

Today, many critical electronic devices, such as health-monitoring sensors [1,2], pace makers [3], spinal stimulators [4], electric pain relievers [5], wireless sensors [6–8], etc., require minimal amounts of power to function. Such devices have, for long time, relied on batteries that have not kept pace with the devices' demands, especially in terms of energy density [9]. In addition, batteries have a finite life span, and require regular replacement or recharging, which, in many of the previously mentioned examples, is a very cumbersome process. In light of such challenges, vibration-based energy harvesting has flourished as a major thrust area of micro power generation. Various devices have been developed to

E-mail address: mdaqaq@clemson.edu

0022-460X/$ - see front matter © 2010 Elsevier Ltd. All rights reserved.
doi:10.1016/j.jsv.2010.04.002

transform mechanical motions directly into electricity by exploiting the ability of active materials and some mechanisms to generate an electric potential in response to mechanical stimuli and external vibrations [10–12].

However, there are still two major issues limiting the efficiency of energy harvesters. First, traditional *linear* energy harvesters have a very narrow frequency bandwidth and, hence, operate efficiently *only* when the excitation frequency is very close to the fundamental frequency of the harvester. Small variations in the excitation frequency around the harvester's fundamental frequency drops its small energy output even further making the energy harvesting process inefficient. Second, most environmental excitations have a broad-band or time-dependent characteristics in which the energy is distributed over a wide spectrum of frequencies or the dominant frequencies vary with time. Together, these two factors have a negative influence that reduces the output power and hinders the efficiency of the harvester.

To resolve these two issues, a large portion of the energy harvesting research is currently directed towards designing harvesters capable of scavenging energy from non-stationary and random excitations [13–21]. One proposed solution is based on purposefully introducing nonlinearities into the harvester's dynamics [22–24]. A class of such harvesters utilizes a nonlinear compliance to extend the coupling between the environmental excitation and the harvester to a wider range of frequencies. The nonlinearities can be introduced using nonlinear magnetic levitation [18,20], Fig. 1(b), or by other design means [25], Fig. 1(a).

In general, such harvesters can be modeled as a uni-modal duffing oscillator whose equation of motion can be written as

$$\ddot{x}+2\zeta_{\mathrm{eff}}\dot{x}+x+\beta x^3=F(t) \tag{1}$$

where x denotes the displacement, ζ_{eff} is an effective damping ratio that accounts for both electrical and mechanical damping, $\beta>0$ is a stiffness nonlinearity coefficient, and $F(t)$ is an external excitation. When the excitation is harmonic with a fixed frequency, the nonlinearity bends the steady-state frequency-response curves towards larger frequencies as shown in Fig. 2(a). Consequently, the coupling between the excitation and the harvester is extended to a wider frequency range. In addition, as a result of the nonlinearity, a region of multiple solutions is born. Specifically, for a certain range of frequencies, three branches of solutions co-exist. It is still not clear how the presence of such regions of multiple solutions influences the performance of the harvester especially under random and indeterministic excitations.

A quick look at the power spectral density curves of $x(t)$ under White Gaussian excitations, see Fig. 2(b), reveals that the nonlinearity causes the spectral amplitude to decrease, shifts the peaks towards larger frequencies, and broadens the spectral response. To investigate the implications of these effects on the expected value of the output power, this effort aims at delineating the role that stiffness-type nonlinearities play in energy harvesting under random forced excitations. Specifically, we want to understand whether the broadening of the spectral density curves can aid in the transduction of energy harvesters under realistic excitations and whether the common steady-state fixed-frequency analysis currently

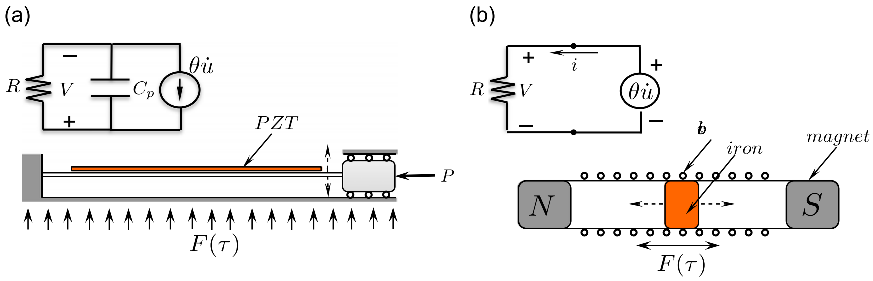

Fig. 1. Schematics of two uni-modal duffing-type harvesters.

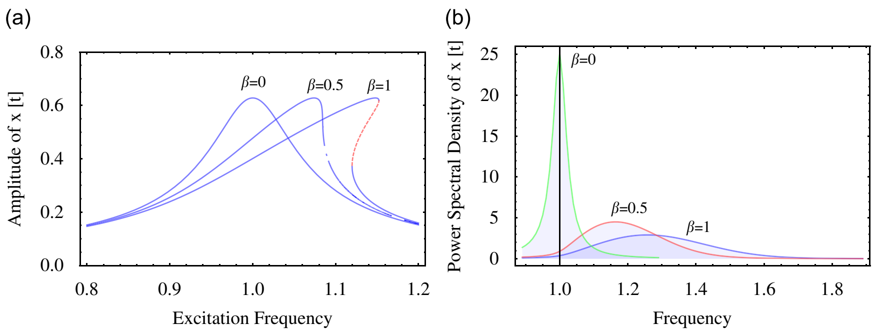

Fig. 2. (a) Steady-state frequency response curves of Eq. (1) under harmonic excitations of a fixed frequency and (b) power spectral density curves of $x(t)$ under White Gaussian excitations of a fixed spectral density.

adopted in the literature is a valid performance indicator. Towards that end, this paper investigates how the statistical characteristics of the output power are affected by the statistics (e.g. bandwidth, and center frequency) of the excitation as well as the nonlinearity. The rest of the paper is organized as follows: In Section 2, we obtain an analytical expression for the expected value of the power under White Gaussian excitations by solving the Fokker–Plank–Kolmogorov (FPK) equation for the exact probability density function (PDF) of the response. In Section 3, we use the Van Kampen expansion to generate a set of linearly coupled ordinary differential equations governing the evolution of the response statistics under Colored excitations. In Section 4, we solve the equations and study the influence of the excitation bandwidth and center frequency on the expected value of the power. Finally, in Section 5, we present our conclusions and recommendations for future work.

2. Response to White Gaussian excitations

We consider an electromagnetic duffing-type harvester, similar to the one shown in Fig. 1(b). This device was proposed by Mann and Sims [18] in the context of energy harvesting using a nonlinear compliance. However, in contrast to [18], we consider the case of forced vibration rather than seismic or base excitation. The equations governing the motion can be expressed as

$$\ddot{u}+2\zeta\omega_n\dot{u}+\omega_n^2u+\theta i+\beta u^3=F(t)$$

$$\theta\dot{u}=iR \tag{2}$$

where u represents the position of the mass, ζ is the mechanical damping ratio, ω_n is the natural frequency, β is a cubic nonlinearity coefficient, θ is an electromechanical coupling coefficient, R is the load resistance, and i is the current passing through the load. It is worth noting that Equation (2) can be used to represent the dynamics under base excitations if u is considered to be the relative displacement and $F(t)$ to be the base acceleration. The force $F(t)$ is assumed to be a Gaussian White noise process with zero mean and autocorrelation function

$$\langle F(t)F(t+\tau)\rangle=2\pi S_0\delta(\tau) \tag{3}$$

where $\langle\ \rangle$ denotes the expected value, S_0 is the spectral density of the excitation, and δ is the dirac-delta function. Without loss of generality, we can assume that all the parameters in the equation are non-dimensional. To obtain an analytical expression for the expected value of the output power, we cast the problem in the Itô stochastic differential form where Eq. (2) can be rewritten as [26]

$$\mathrm{d}x_1=x_2\,\mathrm{d}t$$

$$\mathrm{d}x_2=-\{c_{\mathrm{eff}}x_2+\omega_n^2x_1+\beta x_1^3\}\,\mathrm{d}t+S\,\mathrm{d}B \tag{4}$$

where x_1=u, $x_2=\dot{u}$, $c_{\mathrm{eff}}=2\zeta\omega_n+\theta^2/R$, $S=\pi S_0$, and B is a Brownian motion process such that $\mathrm{d}F/\mathrm{d}t=B(t)$. The joint PDF, $P(x_1, x_2, t)$, of the response can be obtained by solving the linear diffusion FPK equation which can be expressed for system (4) as [27]

$$\frac{\partial P}{\partial t}=-\frac{\partial}{\partial x_1}(x_2P)+\frac{\partial}{\partial x_2}(\{c_{\mathrm{eff}}x_2+\omega_n^2x_1+\beta x_1^3\}P)+S\frac{\partial^2P}{\partial x^2} \tag{5}$$

subjected to the boundary conditions $P(-\infty,t)=P(\infty,t)=0$. While an analytical solution of Eq. (5) is not attainable in the general sense; a stationary solution can be obtained by sitting $\partial P/\partial t$ equal to zero. In such case, Eq. (5) admits a solution of the form:

$$P(x_1,x_2,t)=P_1(x_1,t)\times P_2(x_2,t)=A_1\exp\left\{-\frac{c_{eff}}{2S}\left(\omega_n^2x_1^2+\frac{\beta}{2}x_1^4\right)\right\}\times A_2\exp\left\{-\frac{c_{eff}}{2S}x_2^2\right\} \tag{6}$$

where the normalization constants A_1 and A_2 are given by

$$A_1^{-1}=\int_{-\infty}^{\infty}\exp\left\{-\frac{c_{eff}}{2S}\left(\omega_n^2x_1^2+\frac{\beta}{2}x_1^4\right)\right\}\mathrm{d}x_1,\quad A_2^{-1}=\int_{-\infty}^{\infty}\exp\left\{-\frac{c_{eff}}{2S}x_2^2\right\}\mathrm{d}x_2 \tag{7}$$

Note that the stationary PDF of the response is factored into a function of the displacement, x_1, and a function of the velocity, x_2. This implies that x_1 and x_2 are independent random variables with the PDF of x_2 being independent of the nonlinearity coefficient, β. With that, the expected value of the mean square velocity can be obtained using

$$\langle\dot{u}^2\rangle=\langle x_2^2\rangle=\int_{-\infty}^{\infty}x_2^2P_2(x_2,t)\,\mathrm{d}x_2=\frac{S}{c_{\mathrm{eff}}} \tag{8}$$

From Eqs. (2) and (8), the expected valued of the mean square output current passing through the load can be written as

$$\langle i^2\rangle=\frac{\theta}{R}\langle x_2^2\rangle=\frac{\theta S}{Rc_{\mathrm{eff}}} \tag{9}$$

and the expected value of the power (mean power) is

$$\langle \mathcal{P} \rangle = \frac{\theta S}{c_{\text{eff}}} \tag{10}$$

Eq. (10) can be used to determine the mean output power of a duffing-type harvester under White Gaussian excitations. The resulting expression depends only on the electromechanical coupling coefficient, θ, the excitation's spectral density, S, and the effective damping in the system, c_{eff}. This clearly indicates that the expected value of the power is not a function of the nonlinearity and is equal to that resulting from a linear harvester with $\beta = 0$. Consequently, under White Gaussian excitations of similar spectral densities, both a linear and a uni-modal duffing-type harvester produce the same mean output power.

The stationary PDF of the response given by Eq. (6) also suggests that in order to alter the value of the mean square velocity, and hence power, from the linear case, one should seek other types of nonlinearities. For instance, damping-type nonlinearities that are function of the velocity, x_2, can alter the velocity part of the joint PDF, $P_2(x_2,t)$, which, in turn, may improve the output power depending on the sign and order of the nonlinearity. Inertia nonlinearities and nonlinearities that depend on the velocity and displacement together will make the PDF inseparable and hence are also expected to alter the mean power. With these findings, the question remains whether such nonlinearities can be physically introduced into the dynamics of an actual energy harvesting device.

3. Response to Colored excitations

While many environmental excitations exhibit the characteristics of White excitations, many others have most of their energy trapped within a narrow bandwidth possessing the characteristics of a narrow-band (Colored) excitation. To analyze the influence of the center frequency, bandwidth, and variance of such excitations on the output power of the harvester considered, we couple Eqs. (2) with a second-order filter according to

$$\ddot{F} + \gamma \dot{F} + \omega_c^2 F = N(t) \tag{11}$$

where ω_c is the center frequency of the filter and hence the excitation, γ is its bandwidth, $N(t) = \gamma^{1/2}\omega_c W(t)$, and $W(t)$ is a White Gaussian excitation of a spectral density, S_0, and a correlation function $\langle W(t)W(t+\tau) \rangle = 2\pi S_0 \delta(\tau)$. With this choice of $N(t)$, the spectrum of $F(t)$ can be written as

$$|F(\omega)|^2 = \frac{\gamma \omega_c^2 S_0}{(\omega_c^2 - \omega^2)^2 + \omega^2 \gamma^2} \tag{12}$$

As shown in Fig. 3, for the spectrum shown, the area under the $|F|^2 - \omega$ curve remains constant regardless of the choice of γ and ω_c. In other words, the variance of $F(t)$, $\langle F^2 \rangle = \pi S_0$, is independent of the filter's bandwidth and the center frequency. This is essential for the purpose of comparing the mean power under Colored excitations of different bandwidths and center frequencies.

Again, to find an expression for the mean power, we cast the problem in the Itô stochastic form as

$$\mathrm{d}x_1 = x_2 \, \mathrm{d}t$$

$$\mathrm{d}x_2 = (-c_{\text{eff}} x_2 - \omega_n^2 x_1 - \beta x_1^3 + x_3) \, \mathrm{d}t$$

$$\mathrm{d}x_3 = x_4 \, \mathrm{d}t$$

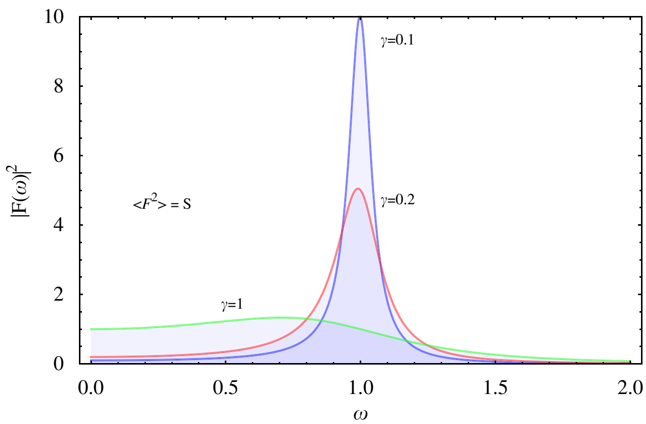

Fig. 3. Power spectrum of $F(t)$ for different bandwidths.

$$dx_4 = (-\gamma x_4 - \omega_c^2 x_3)\,dt + \gamma^{1/2}\omega_c S\,dB \tag{13}$$

where $[x_1,x_2,x_3,x_4] = [u,\dot{u},F,\dot{F}]$. With that, the joint PDF, $P(x_1, x_2, x_3, x_4, t)$, of the response can be obtained by solving the linear diffusion FPK equation which can be expressed for system (13) as

$$\frac{\partial P}{\partial t} = -\frac{\partial}{\partial x_1}\{x_2 P\} + \frac{\partial}{\partial x_2}\{P(c_{\mathrm{eff}} x_2 + \omega_n^2 x_1 + \beta x_1^3 - x_3)\} - \frac{\partial}{\partial x_3}\{x_4 P\} + \frac{\partial}{\partial x_4}\{P(\gamma x_4 + \omega_c^2 x_3)\} + \alpha S \frac{\partial^2 P}{\partial^2 x_4} \tag{14}$$

subjected to the boundary conditions $P(-\infty,t) = P(\infty,t) = 0$. Here $\alpha = \gamma\omega_c^2$. Even in the steady-state case, an exact solution of Eq. (14) is not attainable. For small nonlinearities and mean square values of the x_i's, we can use the Van Kampen expansion [28] to obtain an approximate solution of Eq. (14). In the Van Kampen expansion, which was introduced in the context of some statistical physics problem, the variables are expanded in a successive powers of the excitation's spectral density S. That is,

$$x_1 = S^{1/2}\eta_1 + \mathcal{O}(S^{3/2})$$

$$x_2 = S^{1/2}\eta_2 + \mathcal{O}(S^{3/2})$$

$$x_3 = S^{1/2}\eta_3 + \mathcal{O}(S^{3/2})$$

$$x_4 = S^{1/2}\eta_4 + \mathcal{O}(S^{3/2}) \tag{15}$$

The reason for expanding x_i in orders of $S^{1/2}$ stems from our previous knowledge that mean square value of x_i or $\langle x_i^2 \rangle$, which is a measure of the response amplitude, will turn out to be proportional to S. With this expansion, the PDF becomes a function of the new variables η_i as

$$P(x_1,x_2,x_3,x_4,t) = P(S^{1/2}\eta_1, S^{1/2}\eta_2, S^{1/2}\eta_3, S^{1/2}\eta_4, t) = G(\eta_1,\eta_2,\eta_3,\eta_4,t) \tag{16}$$

In terms of the new PDF, the FPK equation becomes

$$\frac{\partial G}{\partial t} = -\eta_2\frac{\partial G}{\partial \eta_1} + \frac{\partial G}{\partial \eta_2}\{\omega_n^2\eta_1 + \beta S\eta_1^3 - \eta_3\} + c_{\mathrm{eff}}\frac{\partial}{\partial \eta_2}\{G\eta_2\} - \eta_4\frac{\partial G}{\partial \eta_3} + \omega_c^2\eta_3\frac{\partial G}{\partial \eta_4} + \alpha\frac{\partial^2 G}{\partial^2 \eta_4} + \mathcal{O}(S^{3/2}) \tag{17}$$

subjected to the boundary conditions $G(-\infty,t) = G(\infty,t) = 0$. Next, we generate the equations governing the response statistics (statistical moments). For a general function $\Phi(\eta_1,\eta_2,\eta_3,\eta_4)$, the response statistics, $\langle \Phi \rangle$, can be obtained by multiplying both sides of Eq. (17) by Φ and integrating by parts over the entire space; that is

$$\begin{aligned}&\int_{-\infty}^{\infty}\int_{-\infty}^{\infty}\int_{-\infty}^{\infty}\int_{-\infty}^{\infty}\Phi\frac{\partial G}{\partial t}\,d\eta_1\,d\eta_2\,d\eta_3\,d\eta_4\\ &= \int_{-\infty}^{\infty}\int_{-\infty}^{\infty}\int_{-\infty}^{\infty}\int_{-\infty}^{\infty}\Phi\left\{-\eta_2\frac{\partial G}{\partial \eta_1} + \frac{\partial G}{\partial \eta_2}\{\omega_n^2\eta_1 + \beta S\eta_1^3 - \eta_3\} + c_{\mathrm{eff}}\frac{\partial}{\partial \eta_2}\{G\eta_2\} - \eta_4\frac{\partial G}{\partial \eta_3} + \omega_c^2\eta_3\frac{\partial G}{\partial \eta_4} + \alpha\frac{\partial^2 G}{\partial^2 \eta_4}\right\}d\eta_1\,d\eta_2\,d\eta_3\,d\eta_4\end{aligned} \tag{18}$$

For the sake of illustration, we obtain the expected mean square value of variable η_1, i.e., $\Phi = \eta_1^2$. In that case, we can write

$$\begin{aligned}&\int_{-\infty}^{\infty}\int_{-\infty}^{\infty}\int_{-\infty}^{\infty}\int_{-\infty}^{\infty}\eta_1^2\frac{\partial G}{\partial t}\,d\eta_1\,d\eta_2\,d\eta_3\,d\eta_4\\ &= \int_{-\infty}^{\infty}\int_{-\infty}^{\infty}\int_{-\infty}^{\infty}\int_{-\infty}^{\infty}\eta_1^2\left\{-\eta_2\frac{\partial G}{\partial \eta_1} + \frac{\partial G}{\partial \eta_2}\{\omega_n^2\eta_1 + \beta S\eta_1^3 - \eta_3\} + c_{\mathrm{eff}}\frac{\partial}{\partial \eta_2}\{G\eta_2\} - \eta_4\frac{\partial G}{\partial \eta_3} + \omega_c^2\eta_3\frac{\partial G}{\partial \eta_4} + \alpha\frac{\partial^2 G}{\partial^2 \eta_4}\right\}d\eta_1\,d\eta_2\,d\eta_3\,d\eta_4\end{aligned} \tag{19}$$

The left-hand side of the equation can be rewritten as

$$\int_{-\infty}^{\infty}\int_{-\infty}^{\infty}\int_{-\infty}^{\infty}\int_{-\infty}^{\infty}\eta_1^2\frac{\partial G}{\partial t}\,d\eta_1\,d\eta_2\,d\eta_3\,d\eta_4 = \frac{\partial}{\partial t}\int_{-\infty}^{\infty}\int_{-\infty}^{\infty}\int_{-\infty}^{\infty}\int_{-\infty}^{\infty}\eta_1^2 G\,d\eta_1\,d\eta_2\,d\eta_3\,d\eta_4 = \frac{d}{dt}\langle \eta_1^2 \rangle \tag{20}$$

The right-hand side can be integrated by parts. Since the boundary conditions on the FPK equation are identically zero; all the terms except the first one vanish upon integration. This leads to

$$\begin{aligned}\frac{d}{dt}\langle \eta_1^2 \rangle &= -\int_{-\infty}^{\infty}\int_{-\infty}^{\infty}\int_{-\infty}^{\infty}\int_{-\infty}^{\infty}\eta_1^2\eta_2\frac{\partial G}{\partial \eta_1}\,d\eta_1\,d\eta_2\,d\eta_3\,d\eta_4\\ &= -\eta_1^2\eta_2 G|_{-\infty}^{\infty} + 2\int_{-\infty}^{\infty}\int_{-\infty}^{\infty}\int_{-\infty}^{\infty}\int_{-\infty}^{\infty}\eta_1\eta_2 G\,d\eta_1\,d\eta_2\,d\eta_3\,d\eta_4 = 2\langle \eta_1\eta_2 \rangle\end{aligned} \tag{21}$$

In a similar manner, we generate the equations governing the other response statistics. Keeping only moments up to fourth order, we obtain 45 linearly coupled equations that need to be solved together. These equations are listed in Appendix A.

4. Results and discussion

4.1. Effect of the excitation's bandwidth

To analyze the effect of the excitation's bandwidth on the expected stationary value of the power, $\langle \mathcal{P} \rangle$, we study variation of the stationary mean square velocity, $\langle x_2^2 \rangle$, (proportional to the power), with the nonlinearity for different bandwidths. To that end, we set the time derivatives in the equations governing the response statistics to zero and solve the resulting 45 linearly coupled algebraic equations for the stationary response statistics. Fig. 4 depicts variation of $\gamma\langle x_2^2 \rangle$ with the nonlinearity coefficient β for an excitation centered at the natural frequency of the harvester, i.e. $\omega_c = \omega_n$. We note that, for large bandwidths approaching the White excitation limit, the mean square velocity and hence power are insensitive to variations in the nonlinearity. This corroborates the results of Eq. (8). For the parameters used in the simulations, the expected value of the velocity as calculated using Eq. (8) is $\langle x_2^2 \rangle = 1$. This represents the limit which the curves of Fig. 4 approach when γ approaches infinity.

For smaller bandwidths, the expected value of the power becomes sensitive to variations in the nonlinearity coefficient. Indeed, Fig. 4 demonstrates that the mean power decreases as the nonlinearity increases indicating that the nonlinearity does not improve the output power even when the excitations are Colored. In other words, best harvester's performance is always attained when $\beta = 0$. Long-time numerical integration of the governing equations using the Stochastic Communication Toolbox in Matlab reveals good agreement with the Van Kampen expansion for large bandwidths and small nonlinearities. As the bandwidth decreases, especially for large nonlinearities, more deviations are pronounced. This can be attributed to the fact that, as the bandwidth gets smaller, the variance of x_1 and x_2 increases significantly and the one term Van Kampen expansion adopted here becomes inaccurate.

To study the effect of the nonlinearity on the output power for random excitations having very small bandwidths, we revert to a long-time integration scheme where the governing equation are integrated for a very long time (approximately 100 000 T, where T is the response period). The expected mean square value of x_2 is then obtained numerically and normalized by the expected mean square value of the excitation x_3. This normalization is necessary because, unlike the Van Kampen expansion where $\langle x_3^2 \rangle$ is guaranteed to be constant; $\langle x_3^2 \rangle$ varies as β is changed in the numerical scheme. We kept these variations to less than 1 percent of the nominal value by integrating for a longer periods of time. Fig. 5 depicts variation of $\langle x_2^2 \rangle / \langle x_3^2 \rangle$ with β for $\gamma = 0.05$. Again, we can clearly see that the nonlinearity causes the expected value of the output power to drop significantly when compared to the linear harvester.

4.2. Effect of the excitation's center frequency

Since the steady-state response-frequency curves under deterministic excitations bend to the right as the nonlinearity increases, it may be beneficial to tune the excitation's center frequency to a frequency that is larger than the natural one. To investigate this argument, Fig. 6 depicts variation of the mean square velocity with the nonlinearity coefficient for different center frequencies and $\gamma = 1$. It can be seen that, in general, when the bandwidth is large, the trend of the mean power decreasing with the nonlinearity continues even for excitations that are not centered at the natural frequency of the harvester. Furthermore, as expected, the mean value of the power increases with ω_c. As such, it can be beneficial to tune energy harvesters with inherent stiffness-type nonlinearities to a frequency that is slightly larger then the natural frequency when the nonlinearity is of the hardening nature, and to a frequency that is slightly less then the natural frequency for softening nonlinearities. We also note that, when $\beta = 0$, the expected value of the output power is slightly

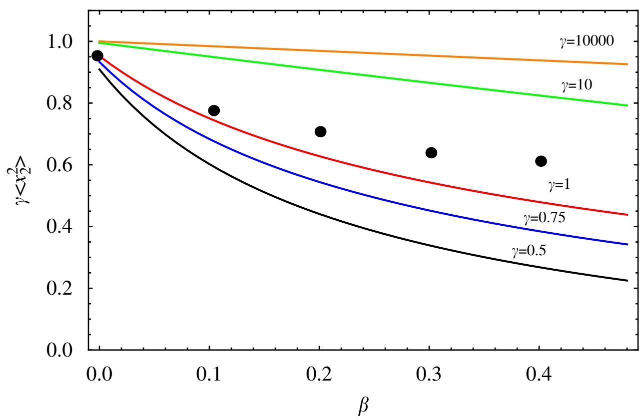

Fig. 4. Variation of the mean square velocity with the nonlinearity coefficient β for different values of γ. Results are obtained for c_{eff}=0.05, S=0.05, $\omega_n = 1$, and $\omega_c = 1$. Circles represent solutions obtained via long time integration (100 000 T where T is the response period) of the equations of motion at $\gamma = 1$. The integration was carried using the stochastic communication toolbox in Matlab.

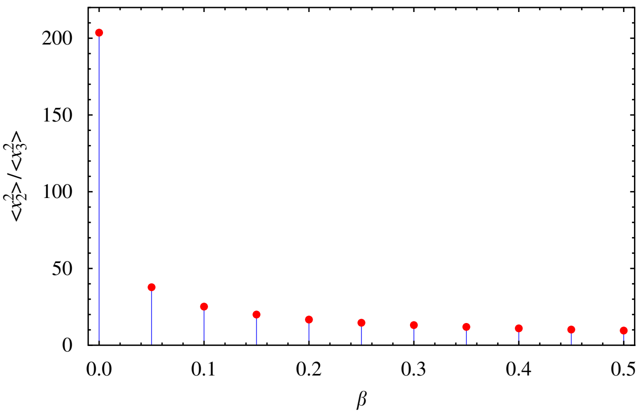

Fig. 5. Variation of the mean square velocity with the nonlinearity coefficient β for $\gamma = 0.05$. Results are obtained for c_{eff}=0.05, S=0.05, $\omega_n = 1$, and $\omega_c = 1$.

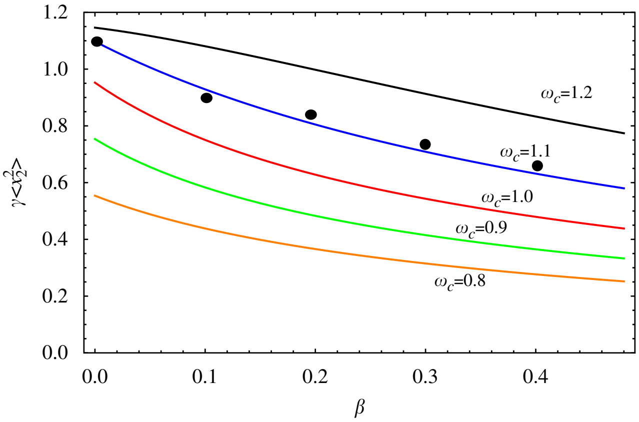

Fig. 6. Variation of the mean square velocity with the nonlinearity coefficient β for different values of ω_c. Results are obtained for c_{eff}=0.05, S=0.05, $\omega_n = 1$, and $\gamma = 1$. Circles represent solutions obtained via long time integration (100 000 T) of the equations of motion at $\omega_c = 1.1$. The integration was carried using the stochastic communication toolbox in Matlab.

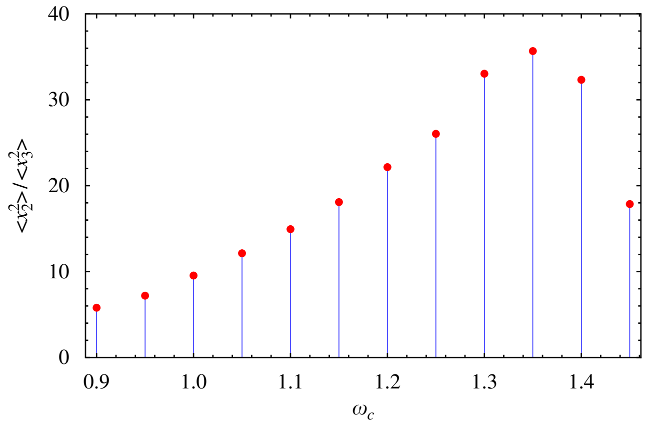

Fig. 7. Variation of the mean square velocity normalized with respect to the mean square excitation with the center frequency ω_c. Results are obtained for c_{eff}=0.05, S=0.05, $\omega_n = 1$, $\gamma = 0.05$, and $\beta = 0.5$.

larger for larger ω_c's. This phenomenon, however, has nothing to do with power enhancement and occurs only because of the nature of the second-order filter used to simulate the excitation. Specifically, because the peak in the excitation spectrum shifts towards lower frequencies as γ increases, the mean output power increases when the center frequency of the excitation is shifted towards larger frequencies.

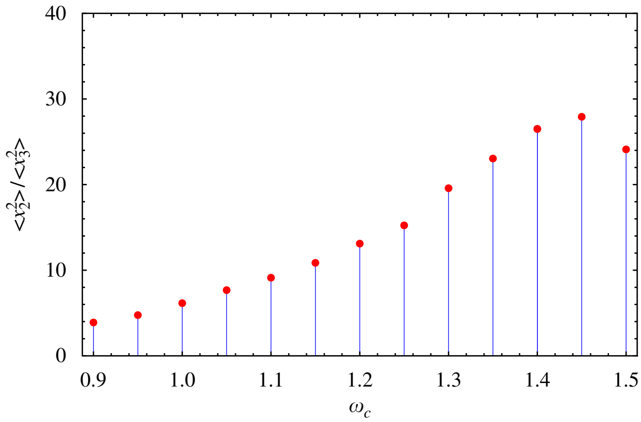

Fig. 8. Variation of the mean square velocity normalized with respect to the mean square excitation with the center frequency ω_c. Results are obtained for c_{eff}=0.05, S=0.05, $\omega_n = 1$, $\gamma = 0.05$, and $\beta = 1$.

To investigate the influence of the excitation's center frequency for smaller bandwidths, we use long-time integration to study variation of the $\langle x_2^2 \rangle / \langle x_3^2 \rangle$ with the center frequency for $\gamma = 0.05$ and $\beta = 0.5$ as shown in Fig. 7. It can be seen that the peak in the expected value does not occur at $\omega_c = 1$ but rather at a larger value, approximately $\omega_c = 1.35$ for this simulation. Again, this indicates that, for energy harvesters having nonlinearities in the compliance, it can be beneficial to tune the harvester at larger frequencies depending on the value of the nonlinearity and bandwidth of the excitation. For the same bandwidth and a larger nonlinearity, $\beta = 1$, the expected value of the power decreases and the peak response shifts towards an even larger frequency, $\omega_c = 1.45$, see Fig. 8. This reinforces the conclusion that the mean power decreases with the nonlinearity even for smaller bandwidths. It is also worth noting that the peak values obtained at the optimal ω_c for the nonlinear harvesters remain much smaller than those obtained for a linear harvester whose natural frequency is tuned at the center frequency of the excitation. Indeed, for $\beta = 0$, $\omega_n = \omega_c$ and the same parameters used in the previous simulations, $\langle x_2^2 \rangle / \langle x_3^2 \rangle = 210$. This is approximately 5.5 times that obtained at the optimal ω_c when $\beta = 0.5$ and about 7.5 times that obtained at the optimal ω_c when $\beta = 1$.

5. Conclusions and future work

We studied the response of uni-modal duffing harvesters to Gaussian White and Colored excitations. We showed that the mean output power of the harvester under White excitations is not influenced by stiffness-type nonlinearities. We also demonstrated that other type of nonlinearities such as damping and inertia nonlinearities may be beneficial to the harvester's operation. As such, future efforts should be directed towards incorporating such nonlinearities into the operation concept of energy harvesters. Furthermore, our results show that stiffness-type nonlinearities hinder the efficiency of the harvester under Colored excitations of different bandwidths and center frequencies. Hence, in general, such nonlinearities should be avoided when designing energy harvesters for forced-vibration random environments. Additional work is needed to assess the importance of base-excitation rather than forced-vibration of duffing harvesters. Current work is focused on extending this analysis to bi-modal duffing type harvesters.

Appendix A. Equations governing the response statistics

$$\frac{\mathrm{d}}{\mathrm{d}t}\langle \eta_1^2 \rangle = 2\langle \eta_1\eta_2 \rangle \tag{A.1}$$

$$\frac{\mathrm{d}}{\mathrm{d}t}\langle \eta_2^2 \rangle = -2\omega_n^2\langle \eta_1\eta_2 \rangle - 2\beta S\langle \eta_1^3\eta_2 \rangle + 2\langle \eta_2\eta_3 \rangle - 2c_{\mathrm{eff}}\langle \eta_2^2 \rangle \tag{A.2}$$

$$\frac{\mathrm{d}}{\mathrm{d}t}\langle \eta_3^2 \rangle = 2\langle \eta_3\eta_4 \rangle \tag{A.3}$$

$$\frac{\mathrm{d}}{\mathrm{d}t}\langle \eta_1\eta_2 \rangle = \langle \eta_2^2 \rangle - \omega_n^2\langle \eta_1^2 \rangle - \beta S\langle \eta_1^4 \rangle + \langle \eta_1\eta_3 \rangle - c_{\mathrm{eff}}\langle \eta_1\eta_2 \rangle \tag{A.4}$$

$$\frac{\mathrm{d}}{\mathrm{d}t}\langle \eta_1\eta_3 \rangle = \langle \eta_2\eta_3 \rangle + \langle \eta_1\eta_4 \rangle \tag{A.5}$$

$$\frac{\mathrm{d}}{\mathrm{d}t}\langle \eta_1\eta_4 \rangle = \langle \eta_2\eta_4 \rangle - \gamma\langle \eta_1\eta_4 \rangle - \omega_c^2\langle \eta_1\eta_3 \rangle \tag{A.6}$$

$$\frac{\mathrm{d}}{\mathrm{d}t}\langle \eta_4^2 \rangle = -2\gamma\langle \eta_4^2 \rangle - 2\omega_c^2\langle \eta_3\eta_4 \rangle + 2\alpha \tag{A.7}$$

$$\frac{\mathrm{d}}{\mathrm{d}t}\langle \eta_2\eta_4 \rangle = -\omega_n^2\langle \eta_1\eta_4 \rangle - S\beta\langle \eta_1^3\eta_4 \rangle + \langle \eta_3\eta_4 \rangle - (c_{\mathrm{eff}}+\gamma)\langle \eta_2\eta_4 \rangle - \omega_c^2\langle \eta_2\eta_3 \rangle \tag{A.8}$$

$$\frac{\mathrm{d}}{\mathrm{d}t}\langle \eta_2\eta_3 \rangle = -\omega_n^2\langle \eta_1\eta_3 \rangle - \beta S\langle \eta_1^3\eta_3 \rangle + \langle \eta_3^2 \rangle - c_{\mathrm{eff}}\langle \eta_2\eta_3 \rangle + \langle \eta_2\eta_4 \rangle \tag{A.9}$$

$$\frac{\mathrm{d}}{\mathrm{d}t}\langle \eta_3\eta_4 \rangle = \langle \eta_4^2 \rangle - \gamma\langle \eta_3\eta_4 \rangle - \omega_c^2\langle \eta_3^2 \rangle \tag{A.10}$$

$$\frac{\mathrm{d}}{\mathrm{d}t}\langle \eta_2\eta_1^3 \rangle = 3\langle \eta_1^2\eta_2^2 \rangle - \omega_n^2\langle \eta_1^4 \rangle + \langle \eta_1^3\eta_3 \rangle - c_{\mathrm{eff}}\langle \eta_1^3\eta_2 \rangle \tag{A.11}$$

$$\frac{\mathrm{d}}{\mathrm{d}t}\langle \eta_1^4 \rangle = 4\langle \eta_1^3\eta_2 \rangle \tag{A.12}$$

$$\frac{\mathrm{d}}{\mathrm{d}t}\langle \eta_1^3\eta_4 \rangle = 3\langle \eta_1^2\eta_2\eta_4 \rangle - \gamma\langle \eta_1^3\eta_4 \rangle - \omega_c^2\langle \eta_1^3\eta_3 \rangle \tag{A.13}$$

$$\frac{\mathrm{d}}{\mathrm{d}t}\langle \eta_1^3\eta_3 \rangle = 3\langle \eta_1^2\eta_2\eta_3 \rangle + \langle \eta_1^3\eta_4 \rangle \tag{A.14}$$

$$\frac{\mathrm{d}}{\mathrm{d}t}\langle \eta_1^2\eta_2^2 \rangle = 2\langle \eta_1\eta_2^3 \rangle - 2\omega_n^2\langle \eta_1^3\eta_2 \rangle + 2\langle \eta_1^2\eta_2\eta_3 \rangle - 2c_{\mathrm{eff}}\langle \eta_1^2\eta_2^2 \rangle \tag{A.15}$$

$$\frac{\mathrm{d}}{\mathrm{d}t}\langle \eta_1^2\eta_2\eta_4 \rangle = 2\langle \eta_1\eta_2^2\eta_4 \rangle + \langle \eta_1^2\eta_3\eta_4 \rangle - (\gamma+c_{\mathrm{eff}})\langle \eta_1^2\eta_2\eta_4 \rangle - \omega_c^2\langle \eta_1^2\eta_2\eta_3 \rangle - \omega_n^2\langle \eta_1^3\eta_4 \rangle \tag{A.16}$$

$$\frac{\mathrm{d}}{\mathrm{d}t}\langle \eta_1^2\eta_2\eta_3 \rangle = 2\langle \eta_1\eta_2^2\eta_3 \rangle + \langle \eta_1^2\eta_3^2 \rangle + \langle \eta_1^2\eta_2\eta_4 \rangle - c_{\mathrm{eff}}\langle \eta_1^2\eta_2\eta_3 \rangle - \omega_n^2\langle \eta_1^3\eta_3 \rangle \tag{A.17}$$

$$\frac{\mathrm{d}}{\mathrm{d}t}\langle \eta_1\eta_2^3 \rangle = \langle \eta_2^4 \rangle + 3\langle \eta_1\eta_2^2\eta_3 \rangle - 3c_{\mathrm{eff}}\langle \eta_1\eta_2^3 \rangle - 3\omega_n^2\langle \eta_1^2\eta_2^2 \rangle \tag{A.18}$$

$$\frac{\mathrm{d}}{\mathrm{d}t}\langle \eta_1\eta_2^2\eta_4 \rangle = \langle \eta_2^3\eta_4 \rangle + 2\langle \eta_1\eta_2\eta_3\eta_4 \rangle - (\gamma+2c_{\mathrm{eff}})\langle \eta_1\eta_2^2\eta_4 \rangle - \omega_c^2\langle \eta_1\eta_2^2\eta_3 \rangle - 2\omega_n^2\langle \eta_1^2\eta_2\eta_4 \rangle \tag{A.19}$$

$$\frac{\mathrm{d}}{\mathrm{d}t}\langle \eta_1^2\eta_3\eta_4 \rangle = 2\langle \eta_1\eta_2\eta_3\eta_4 \rangle + \langle \eta_1^2\eta_4^2 \rangle - \gamma\langle \eta_1\eta_2\eta_3\eta_4 \rangle - \omega_c^2\langle \eta_1^2\eta_3^2 \rangle \tag{A.20}$$

$$\frac{\mathrm{d}}{\mathrm{d}t}\langle \eta_1\eta_2^2\eta_3 \rangle = \langle \eta_2^3\eta_3 \rangle + 2\langle \eta_1\eta_2\eta_3^2 \rangle + \langle \eta_1\eta_2^2\eta_4 \rangle - 2c_{\mathrm{eff}}\langle \eta_1\eta_2^2\eta_3 \rangle - 2\omega_n^2\langle \eta_1^2\eta_2\eta_3 \rangle \tag{A.21}$$

$$\frac{\mathrm{d}}{\mathrm{d}t}\langle \eta_1^2\eta_3^2 \rangle = 2\langle \eta_1\eta_2\eta_3^2 \rangle + 2\langle \eta_1^2\eta_3\eta_4 \rangle \tag{A.22}$$

$$\frac{\mathrm{d}}{\mathrm{d}t}\langle \eta_2^4 \rangle = 4\langle \eta_2^3\eta_3 \rangle - 4c_{\mathrm{eff}}\langle \eta_2^4 \rangle - 4\omega_n^2\langle \eta_1\eta_2^3 \rangle \tag{A.23}$$

$$\frac{\mathrm{d}}{\mathrm{d}t}\langle \eta_2^3\eta_4 \rangle = 3\langle \eta_2^2\eta_3\eta_4 \rangle - (\gamma+3c_{\mathrm{eff}})\langle \eta_2^3\eta_4 \rangle - \omega_c^2\langle \eta_2^3\eta_3 \rangle - 3\omega_n^2\langle \eta_1\eta_2^2\eta_4 \rangle \tag{A.24}$$

$$\frac{\mathrm{d}}{\mathrm{d}t}\langle \eta_1\eta_2\eta_3\eta_4 \rangle = \langle \eta_2^2\eta_3\eta_4 \rangle + \langle \eta_1\eta_3^2\eta_4 \rangle + \langle \eta_1\eta_2\eta_4^2 \rangle - (\gamma+c_{\mathrm{eff}})\langle \eta_1\eta_2\eta_3\eta_4 \rangle - \omega_c^2\langle \eta_1\eta_2\eta_3^2 \rangle - \omega_n^2\langle \eta_1^2\eta_3\eta_4 \rangle \tag{A.25}$$

$$\frac{\mathrm{d}}{\mathrm{d}t}\langle \eta_1^2\eta_4^2 \rangle = 2\alpha\langle \eta_1^2 \rangle + 2\langle \eta_1\eta_2\eta_4^2 \rangle - 2\gamma\langle \eta_1^2\eta_4^2 \rangle - 2\omega_c^2\langle \eta_1^2\eta_3\eta_4 \rangle \tag{A.26}$$

$$\frac{\mathrm{d}}{\mathrm{d}t}\langle \eta_2^3\eta_3 \rangle = 3\langle \eta_2^2\eta_3^2 \rangle + \langle \eta_2^3\eta_4 \rangle - 3c_{\mathrm{eff}}\langle \eta_2^3\eta_3 \rangle - 3\omega_n^2\langle \eta_1\eta_2^2\eta_3 \rangle \tag{A.27}$$

$$\frac{\mathrm{d}}{\mathrm{d}t}\langle \eta_1\eta_2\eta_3^2 \rangle = \langle \eta_2^2\eta_3^2 \rangle + \langle \eta_1\eta_3^3 \rangle + 2\langle \eta_1\eta_2\eta_3\eta_4 \rangle - c_{\mathrm{eff}}\langle \eta_1\eta_2\eta_3^2 \rangle - \omega_n^2\langle \eta_1^2\eta_3^2 \rangle \tag{A.28}$$

$$\frac{\mathrm{d}}{\mathrm{d}t}\langle \eta_2^2\eta_3\eta_4 \rangle = 2\langle \eta_2\eta_3^2\eta_4 \rangle + \langle \eta_2^2\eta_4^2 \rangle - (\gamma+2c_{\mathrm{eff}})\langle \eta_2^2\eta_3\eta_4 \rangle - \omega_c^2\langle \eta_2^2\eta_3^2 \rangle - 2\omega_n^2\langle \eta_1\eta_2\eta_3\eta_4 \rangle \tag{A.29}$$

$$\frac{\mathrm{d}}{\mathrm{d}t}\langle \eta_1\eta_3^2\eta_4\rangle = \langle \eta_2\eta_3^2\eta_4\rangle + 2\langle \eta_1\eta_3\eta_4^2\rangle - \gamma\langle \eta_1\eta_3^2\eta_4\rangle - \omega_c^2\langle \eta_1\eta_3^3\rangle \tag{A.30}$$

$$\frac{\mathrm{d}}{\mathrm{d}t}\langle \eta_1\eta_2\eta_4^2\rangle = \langle \eta_2^2\eta_4^2\rangle + \langle \eta_1\eta_3\eta_4^2\rangle - (2\gamma + c_{\mathrm{eff}})\langle \eta_1\eta_2\eta_4^2\rangle - 2\omega_c^2\langle \eta_1\eta_2\eta_3\eta_4\rangle - \omega_n^2\langle \eta_1^2\eta_4^2\rangle + 2\langle \eta_1\eta_2\rangle \tag{A.31}$$

$$\frac{\mathrm{d}}{\mathrm{d}t}\langle \eta_2^2\eta_3^2\rangle = 2\langle \eta_2\eta_3^3\rangle + 2\langle \eta_2^2\eta_3\eta_4\rangle - 2c_{\mathrm{eff}}\langle \eta_2^2\eta_3^2\rangle - 2\omega_n^2\langle \eta_1\eta_2\eta_3^2\rangle \tag{A.32}$$

$$\frac{\mathrm{d}}{\mathrm{d}t}\langle \eta_1\eta_3^3\rangle = \langle \eta_2\eta_3^3\rangle + 3\langle \eta_1\eta_3^2\eta_4\rangle \tag{A.33}$$

$$\frac{\mathrm{d}}{\mathrm{d}t}\langle \eta_2\eta_3^2\eta_4\rangle = \langle \eta_3^3\eta_4\rangle + 2\langle \eta_2\eta_3\eta_4^2\rangle - (\gamma + c_{\mathrm{eff}})\langle \eta_2\eta_3^2\eta_4\rangle - \omega_c^2\langle \eta_2\eta_3^3\rangle - \omega_n^2\langle \eta_1\eta_3^2\eta_4\rangle \tag{A.34}$$

$$\frac{\mathrm{d}}{\mathrm{d}t}\langle \eta_2^2\eta_4^2\rangle = 2\langle \eta_1\eta_3\eta_4^2\rangle - 2(\gamma + c_{\mathrm{eff}})\langle \eta_2^2\eta_4^2\rangle - 2\omega_c^2\langle \eta_2^2\eta_3\eta_4\rangle - 2\omega_n^2\langle \eta_1\eta_2\eta_4^2\rangle + 2\alpha\langle \eta_2^2\rangle \tag{A.35}$$

$$\frac{\mathrm{d}}{\mathrm{d}t}\langle \eta_1\eta_3\eta_4^2\rangle = \langle \eta_2\eta_3\eta_4^2\rangle + \langle \eta_1\eta_4^3\rangle - 2\gamma\langle \eta_1\eta_3\eta_4^2\rangle - 2\omega_c^2\langle \eta_1\eta_3^2\eta_4\rangle + 2\alpha\langle \eta_1\eta_3\rangle \tag{A.36}$$

$$\frac{\mathrm{d}}{\mathrm{d}t}\langle \eta_2\eta_3^3\rangle = \langle \eta_3^4\rangle + 3\langle \eta_2\eta_3^2\eta_4\rangle - c_{\mathrm{eff}}\langle \eta_2\eta_3^3\rangle - \omega_n^2\langle \eta_1\eta_3^3\rangle \tag{A.37}$$

$$\frac{\mathrm{d}}{\mathrm{d}t}\langle \eta_3^3\eta_4\rangle = 3\langle \eta_3^2\eta_4^2\rangle - \gamma\langle \eta_3^3\eta_4\rangle - \omega_c^2\langle \eta_3^4\rangle \tag{A.38}$$

$$\frac{\mathrm{d}}{\mathrm{d}t}\langle \eta_2\eta_3\eta_4^2\rangle = \langle \eta_3^2\eta_4^2\rangle + \langle \eta_2\eta_4^3\rangle - (2\gamma + c_{\mathrm{eff}})\langle \eta_2\eta_3\eta_4^2\rangle - 2\omega_c^2\langle \eta_2\eta_3^2\eta_4\rangle - \omega_n^2\langle \eta_1\eta_3\eta_4^2\rangle + 2\alpha\langle \eta_2\eta_3\rangle \tag{A.39}$$

$$\frac{\mathrm{d}}{\mathrm{d}t}\langle \eta_1\eta_4^3\rangle = \langle \eta_2\eta_4^3\rangle - 3\gamma\langle \eta_1\eta_4^3\rangle - 3\omega_c^2\langle \eta_1\eta_3\eta_4^2\rangle + 6\alpha\langle \eta_1\eta_4\rangle \tag{A.40}$$

$$\frac{\mathrm{d}}{\mathrm{d}t}\langle \eta_3^4\rangle = 4\langle \eta_3^3\eta_4\rangle \tag{A.41}$$

$$\frac{\mathrm{d}}{\mathrm{d}t}\langle \eta_3^2\eta_4^2\rangle = 2\langle \eta_3\eta_4^3\rangle - 2\gamma\langle \eta_3^2\eta_4^2\rangle - 2\omega_c^2\langle \eta_3\eta_4^3\rangle + 2\langle \eta_3^2\rangle \tag{A.42}$$

$$\frac{\mathrm{d}}{\mathrm{d}t}\langle \eta_2\eta_4^3\rangle = \langle \eta_3\eta_4^3\rangle - (3\gamma + c_{\mathrm{eff}})\langle \eta_2\eta_4^3\rangle - 3\omega_c^2\langle \eta_2\eta_3\eta_4^2\rangle - \omega_n^2\langle \eta_1\eta_4^3\rangle + 6\alpha\langle \eta_2\eta_4\rangle \tag{A.43}$$

$$\frac{\mathrm{d}}{\mathrm{d}t}\langle \eta_3\eta_4^3\rangle = \langle \eta_4^4\rangle - 3\gamma\langle \eta_3\eta_4^3\rangle - 3\omega_c^2\langle \eta_3^2\eta_4^2\rangle + 6\alpha\langle \eta_3\eta_4\rangle \tag{A.44}$$

$$\frac{\mathrm{d}}{\mathrm{d}t}\langle \eta_4^4\rangle = -4\gamma\langle \eta_4^4\rangle - 4\omega_c^2\langle \eta_3\eta_4^3\rangle + 12\alpha\langle \eta_4^2\rangle \tag{A.45}$$

References

[1] A.J. duPlessis, M.J. Huigsloot, F.D. Discenzo, Resonant packaged piezoelectric power harvester for machinery health monitoring, *Proceedings of Smart Structures and Materials Conference*, SPIE, San Diego, CA, 2005, p. 5762.

[2] D.J. Inman, B.L. Grisso, Towards autonomous sensing, *Proceedings of Smart Structures and Materials Conference*, SPIE, San Diego, CA, 2006, p. 61740T.

[3] R.S. Sanders, M.T. Lee, Implantable pacemakers, *Proceedings of the IEEE*, vol. 84, no. 3, 1996.

[4] I.D. Capel, H.M. Dorrell, E.P. Spencer, M.W. Davis, The amelioration of the suffering associated with spinal cord injury with subperception transcranial electrical stimulation, *Spinal Cord* 41 (2003) 109–117.

[5] G. Renzenbrink, M.J. Jzerman, Percutaneous neuromuscular electrical stimulation for treating shoulder pain in chronic hemiplegia. Effects on shoulder pain and quality of life, *Clinical Rehabilitation* 18 (2004) 359–365.

[6] S. Roundy, P.K. Wright, J. Rabaey, A study of low level vibrations as a power source for wireless sensor nodes, *Computer Communications* 26 (2003) 1131–1144.

[7] S. Roundy, P.K. Wright, A piezoelectric vibration-based generator for wireless electronics, *Journal of Intelligent Materials and Structures* 16 (2005) 809–823.

[8] S.W. Arms, C.P. Townsend, D.L. Churchill, G.H. Galbreath, S.W. Mundell, Power management for energy harvesting wireless sensors, *Proceedings of the Smart Structures and Materials Conference*, SPIE, San Diego, CA, 2005, pp. 5763, 267–275.

[9] J.A. Paradiso, T. Starner, Energy scavenging for mobile and wireless electronics, IEEE Pervasive Computing 4 (2005) 18–27.

[10] H. Sodano, D.J. Inman, G. Park, A review of power harvesting from vibration using piezoelectric materials, *The Shock and Vibration Digest* 36 (2004) 197–205.

[11] H. Sodano, D.J. Inman, G. Park, Generation and storage of electricity from power harvesting devices, *Journal of Intelligent Material Systems and Structures* 16 (2005) 67–75.

[12] S. Roundy, On the effectiveness of vibration-based energy harvesting, *Journal of Intelligent Materials and Structures* 16 (2005) 809–823.

[13] S. Roundy, Y. Zhang, Toward self-tuning adaptive vibration-based micro-generators, *Smart Materials, Nano- and Micro-Smart Systems*, Sydney, Australia, 2005.
[14] W. Wu, Y. Chen, B. Lee, J. He, Y. Peng, Tunable resonant frequency power harvesting devices, in: *Proceedings of Smart Structures and Materials Conference*, SPIE, San Diego, CA, 2006, p. 61690A.
[15] V. Challa, M. Prasad, Y. Shi, F. Fisher, A vibration energy harvesting device with bidirectional resonance frequency tunability, *Smart Materials and Structures* 75 (2008) 1–10.
[16] S.M. Shahruz, Design of mechanical band-pass filters for energy scavenging, *Journal of Sound and Vibrations* 292 (2006) 987–998.
[17] S.M. Shahruz, Limits of performance of mechanical band-pass filters used in energy harvesting, *Journal of Sound and Vibrations* 294 (2006) 449–461.
[18] B. Mann, N. Sims, Energy harvesting from the nonlinear oscillations of magnetic levitation, *Journal of Sound and Vibrations* 319 (2008) 515–530.
[19] A. Erturk, J. Renno, D. Inman, Modeling of energy harvesting form an L-shaped beam-mass structure with an application to UAVs, *Journal of Intelligent Material Systems and Structures* 20 (2008) 1–16.
[20] D. Barton, S. Burrow, L. Clare, Energy harvesting from vibrations with a nonlinear oscillator, *Proceedings of the ASME 2009 International Design Engineering Technical Conference and Computers and Information in Engineering Conference*, San Diego, CA, 2009.
[21] D. Quinn, D. Vakakis, L. Bergman, Vibration energy harvesting with essential nonlinearities, *Proceedings of the ASME 2007 International Design Engineering Technical Conference and Computers and Information in Engineering Conference*, Las Vegas, NV, 2007.
[22] A. Erturk, J. Hoffman, D.J. Inman, A piezo-magneto-elastic structure for broadband vibration energy harvesting, *Applied Physics Letters* 94 (2009) 254102.
[23] F. Cottone, H. Vocca, L. Gammaitoni, Nonlinear energy harvesting, *Physical Review Letters* 102 (2009) 080601-1–080601-4.
[24] S. Stanton, C. McGehee, B. Mann, Reversible hysteresis for broadband magnetopiezoelastic energy harvesting, *Applied Physics Letters* 95 (2009) 174103.
[25] M.F. Daqaq, New insight into energy harvesting via axially-loaded beams, *Proceedings of the ASME 2009 International Design Engineering Technical Conference and Computers and Information in Engineering Conference*, San Diego, CA, 2009.
[26] K. Ito, Stochastic integral, *Proceedings of the Imperial Academy* (*Tokyo*) 20 (1944) 519–524.
[27] A.H. Jazwinski, *Stochastic Processes and Filtering Theory*, Academic Press, New York, 1970.
[28] R.F. Rodriguez, N.G.V. Kampen, Systematic treatment of fluctuations in a nonlinear oscillator, *Physica A* 85 (1976) 347–362.